



Hydrogen insertion effect on the magnetic properties of $\text{Ce}_2\text{Pd}_2\text{In}$

Wacław Iwasieczko, Dariusz Kaczorowski*

Institute of Low Temperature and Structure Research, Polish Academy of Sciences, Okolna 2, P.O. Box 1410, 50-950 Wrocław, Poland

ARTICLE INFO

Article history:

Received 29 September 2010

Received in revised form 15 October 2010

Accepted 27 October 2010

Available online 4 November 2010

Keywords:

Cerium intermetallics

Hydrogenation

Magnetic properties

ABSTRACT

The effect of hydrogenation on the crystal structure and the magnetic properties of $\text{Ce}_2\text{Pd}_2\text{InH}_x$ was studied up to the hydrogen content $x=4$. In the entire range of x , the system retains the tetragonal unit cell of the parent compound, and nearly isotropic expansion of the crystal lattice was observed for $x \leq 2.5$. Below $x \approx 1.5$, the hydrides exhibit ferromagnetic properties, while at larger hydrogen content antiferromagnetic behaviour was found in samples with the composition up to $x \approx 2.5$. In the entire $\text{Ce}_2\text{Pd}_2\text{InH}_x$ series the magnetic behaviour is governed by the well-localized magnetic moments carried by trivalent cerium ions with fairly stable $4f^1$ electronic configuration.

© 2010 Elsevier B.V. All rights reserved.

1. Introduction

Cerium-based intermetallics continuously attract much attention due to their anomalous physical behaviour that is predominantly governed by interactions between the cerium 4f electrons and non-f electrons of neighbouring atoms, i.e. co-called f-ligand hybridization. It is well known that the f-ligand hybridization is very sensitive to external factors like pressure and magnetic field, but also to changes in atomic environment caused by insertion of hydrogen. The two obvious effects of hydrogenation is crystal lattice expansion and doping with electrons. Both these mechanisms modify the electronic structure of a given system, and thus may influence the strength of f-ligand hybridization, which in turn controls the degree of localization of the 4f-states.

The series of $\text{Ce}_2\text{T}_2\text{In}$ (T=d-electron transition metal) intermetallics is an excellent example of a system in which the f-ligand hybridization entirely controls the electronic ground state properties. Depending on the filling of the transition metal d band, the $\text{Ce}_2\text{T}_2\text{In}$ compounds show well-localized magnetism ($\text{Ce}_2\text{Cu}_2\text{In}$, $\text{Ce}_2\text{Pd}_2\text{In}$, and $\text{Ce}_2\text{Au}_2\text{In}$) or exhibit valence fluctuations ($\text{Ce}_2\text{Ni}_2\text{In}$ and $\text{Ce}_2\text{Rh}_2\text{In}$) [1,2]. Among them, $\text{Ce}_2\text{Pd}_2\text{In}$ was reported to order ferromagnetically at low temperatures [1–8], which is not very often observed for Ce-based compounds. Moreover, in a few reports [1,6,7] the presence of an antiferromagnetic phase located just above the Curie temperature was claimed. The latter feature was clarified in a more recent work [9] to arise due to the effect of nonstoichiometry of the studied specimens. It appeared that some small excess of palladium in $\text{Ce}_2\text{Pd}_2\text{In}$ (nominal composition)

favours antiferromagnetism, whereas excess of cerium stabilises ferromagnetism.

Here we describe the effect of hydrogen insertion into the crystal lattice of ferromagnetic $\text{Ce}_2\text{Pd}_2\text{In}$. This paper is another account on our systematic investigations on hydrogen-induced modifications in the electronic properties of the $\text{Ce}_2\text{T}_2\text{In}$ ternaries, after our recent report on the cerium valence changes in the system $\text{Ce}_2\text{Ni}_2\text{InH}_x$ [10].

2. Experimental

Polycrystalline samples of the parent compound $\text{Ce}_2\text{Pd}_2\text{In}$ were synthesized by arc-melting stoichiometric amounts of the constituents (purity: cerium 99.8%, palladium 99.99%, indium 99.99%) under titanium-gettered argon atmosphere. The buttons were turned over and remelted several times to ensure homogeneity. The weight losses after melting were always smaller than 0.5 mass%. No further heat treatment was given to the ingots. Subsequently, the alloys were crushed into sub-millimetre pieces in an agate mortar under protection of tetrachloroethylene.

Hydrogen absorption experiments were performed in a classical Sievert's-type apparatus adopted for PTC measurements. The samples were placed in a reaction chamber and heated under vacuum (5×10^{-5} Pa) at 473 K for 4 h. After such activation they were cooled down to room temperature and then exposed to hydrogen gas at few atmospheres. The synthesis reaction took place in the temperature range 340–470 K. Attempts to synthesize the $\text{Ce}_2\text{Pd}_2\text{InH}_x$ hydride at higher temperatures resulted in the formation of binary rare-earth hydrides CeH_2 and the appearance of CePdIn as an impurity phase. The given hydrides were cycled *in situ* between room temperature and 473 K several times in order to promote homogeneity. After the synthesis, the samples were slowly cooled down to room temperature at a speed of 3 K/h. The amount of hydrogen in the specimens was determined with the accuracy of ± 0.02 hydrogen atoms per formula unit (H/f.u.) by measuring the hydrogen pressure drop in a calibrated apparatus volume. The residual composition of the hydrides, which showed gradual decomposition as a function of time of exposure to air, was determined by means of complete decomposition of a part of the given sample in an evacuated and calibrated chamber.

All the obtained materials were examined at room temperature by powder X-ray diffraction using a Stoe powder diffractometer with $\text{Cu K}\alpha_1$ radiation and silicon as an internal standard. The unit cell parameters were calculated using the pro-

* Corresponding author. Tel.: +48 71 34 350 21; fax: +48 71 34 410 19.
E-mail address: D.Kaczorowski@int.pan.wroc.pl (D. Kaczorowski).

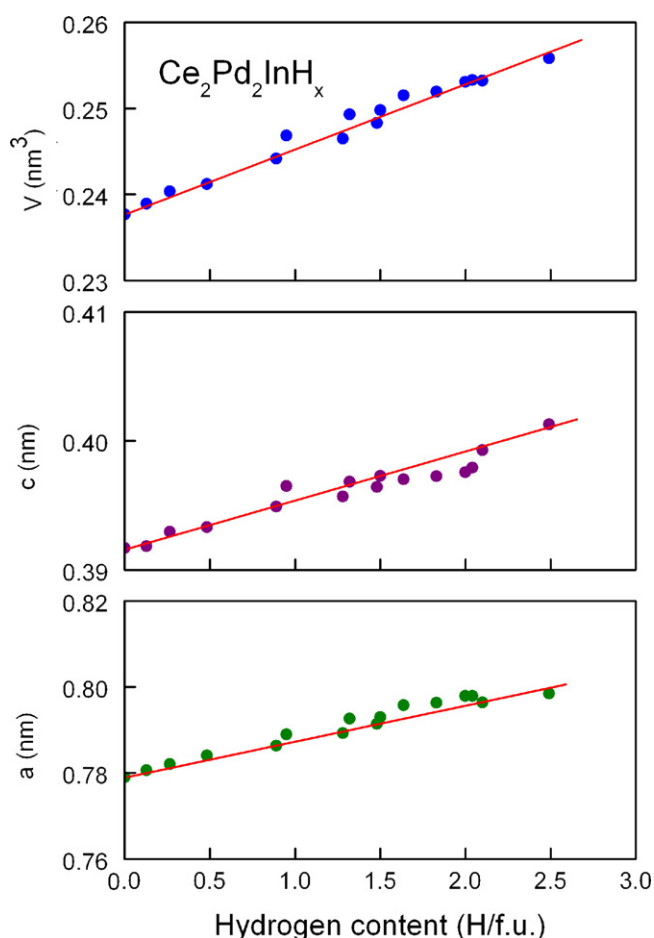


Fig. 1. Variation of the tetragonal lattice parameters a and c , and the unit cell volume V , as a function of the hydrogen content x in the hydrides $\text{Ce}_2\text{Pd}_2\text{InH}_x$ with $x \leq 2.5$. All the data were determined from the X-ray diffraction patterns collected just after removal of the given specimen from the reaction chamber. The straight lines emphasize linear behaviour.

gram DICVOL [11]. Magnetic measurements were performed in the temperature range 1.8–300 K and in applied magnetic fields up to 5 T employing a commercial superconducting quantum interference device (SQUID) magnetometer. For these measurements loose powders were utilized, which were placed in small gelatin capsules.

3. Results and discussion

3.1. Crystal structure

The powder X-ray diffraction patterns of the $\text{Ce}_2\text{Pd}_2\text{InH}_x$ hydrides with $x \leq 2.5$, taken directly after removal from the reaction chamber, showed a close resemblance to that of the parent compound $\text{Ce}_2\text{Pd}_2\text{In}$, with all the Bragg peaks indexable assuming a primitive tetragonal structure of the Mo_2FeB_2 -type (space group $P4/mbm$). The lattice parameters derived for $\text{Ce}_2\text{Pd}_2\text{In}$ were $a = 0.7794(5)$ nm and $c = 0.3917(4)$ nm, in good agreement with the values reported previously [1–9]. As demonstrated in Fig. 1, hydrogenation brings about almost linear increases of both lattice parameters. The observed expansion of the unit cell is nearly isotropic, characterized by $\Delta a/a = 1.14\%$ and $\Delta c/c = 1.16\%$ ($\Delta V/V = 3.6\%$) per one hydrogen atom. Such behaviour suggests that the hydrogen atoms in $\text{Ce}_2\text{Pd}_2\text{InH}_x$ randomly occupy interstitial sites in the crystal lattice. Interestingly, distinctly anisotropic expansion of the unit cell was found for the $\text{Ce}_2\text{Ni}_2\text{InH}_x$ [10] and $\text{Ce}_2\text{Cu}_2\text{InH}_x$ [12] series, with the major contribution along the tetragonal c -axis.

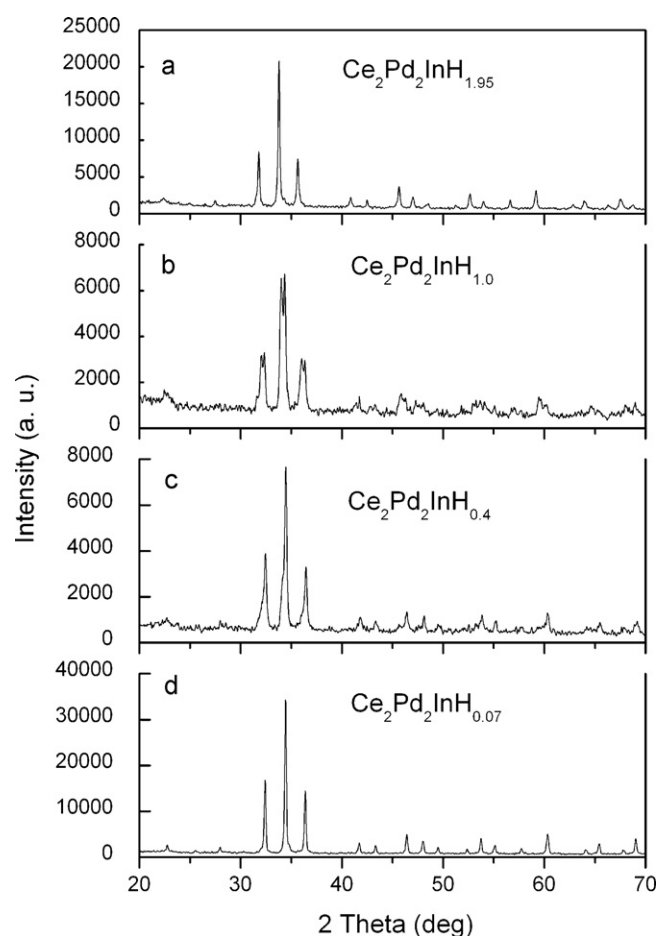


Fig. 2. Powder X-ray diffraction patterns of $\text{Ce}_2\text{Pd}_2\text{InH}_{1.95}$ collected after (a) 10 min, (b) one day, (c) two days, and (d) one week of exposition of the sample to air. The hydrogen content indicated in the panels (b) and (c) was estimated from the relative peak intensities due to the phases with the terminal compositions.

All the prepared $\text{Ce}_2\text{Pd}_2\text{InH}_x$ hydrides were found to be unstable against time. As an example, Fig. 2 presents the X-ray pattern of $\text{Ce}_2\text{Pd}_2\text{InH}_{1.95}$ taken just after the synthesis and the patterns measured after some time of exposure to air. Clearly, the sample spontaneously decomposes (note the weighted coexistence of two tetragonal phases in panels (b) and (c) that correspond to the initial and final compositions) and after one week it contains only minute amount of hydrogen. Remarkably, the X-ray pattern of the latter phase consists of sharp Bragg peaks located at the 2θ positions almost equal to those of pure $\text{Ce}_2\text{Pd}_2\text{In}$. A likely reason for the observed behaviour is small enthalpy of formation of the $\text{Ce}_2\text{Pd}_2\text{InH}_x$ hydrides. In this context it is worthwhile mentioning that the equilibrium hydrogen pressure above the $\text{Ce}_2\text{Pd}_2\text{InH}_{1.95}$ hydride at room temperature was estimated to be as low as about 0.01 MPa.

The powder X-ray patterns of the $\text{Ce}_2\text{Pd}_2\text{InH}_x$ samples with $x > 2.5$ reveal the presence of some amount of impurity phases CeH_2 and CePdIn (see an example in Fig. 3a), and the quantity of the binary hydride increases with increasing hydrogen content. In contrast to the afore-discussed alloys with smaller hydrogen content, upon decomposition of these hydrides by heating to 770 K the parent material is not fully recovered, i.e. the CePdIn impurity remains visible. The hydride with largest x , reached in this study, was $\text{Ce}_2\text{Pd}_2\text{InH}_{4.0}$, yet this material appeared quite amorphous (see Fig. 3b).

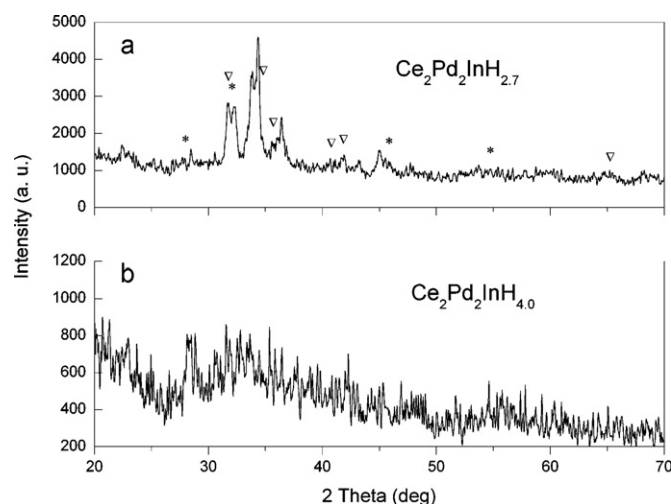


Fig. 3. Powder X-ray diffraction pattern of (a) $\text{Ce}_2\text{Pd}_2\text{InH}_{2.7}$ and (b) $\text{Ce}_2\text{Pd}_2\text{InH}_{4.0}$ obtained on samples freshly taken out of the reactor. The stars and triangles in the panel (a) denote the Bragg peaks due to the CeH_2 and CePdIn impurity phase, respectively.

3.2. Magnetic properties

The starting material used for the fabrication of all the hydrides studied in this work was a single-phase ferromagnetic “ $\text{Ce}_2\text{Pd}_2\text{In}$ ”. As demonstrated in Fig. 4, no trace of any antiferromagnetic component was observed above T_C , even in very weak magnetic fields (compare Fig. 8 in Ref. [1]). Thus, according to Ref. [9], our sample was likely slightly nonstoichiometric, located in the Ce-rich region of the homogeneity field formed by two branches $\text{Ce}_{2+x}\text{Pd}_{1.85}\text{In}_{1-x}$ and $\text{Ce}_{1.95}\text{Pd}_{2+2x}\text{In}_{1-x}$, in the very vicinity of the ideal composition $\text{Ce}_2\text{Pd}_2\text{In}$ (therefore this formula is used in the following). The Curie temperature, defined as an inflection point on the $\sigma(T)$ curve, is $T_C = 4.6(1)\text{ K}$, i.e. it is somewhat higher than those reported in the literature [1–9]. The scatter in the literature data likely arises from small differences in the actual compositions of the studied materials.

Magnetic measurements performed for several $\text{Ce}_2\text{Pd}_2\text{InH}_x$ compounds with various hydrogen content (the experiments were made just after removal of a given specimen from the reaction chamber, in parallel with X-ray examinations of a part of same sample) revealed that all the hydrides with $x < 1.48$ exhibit a ferromagnetic ground state. The Curie temperature in

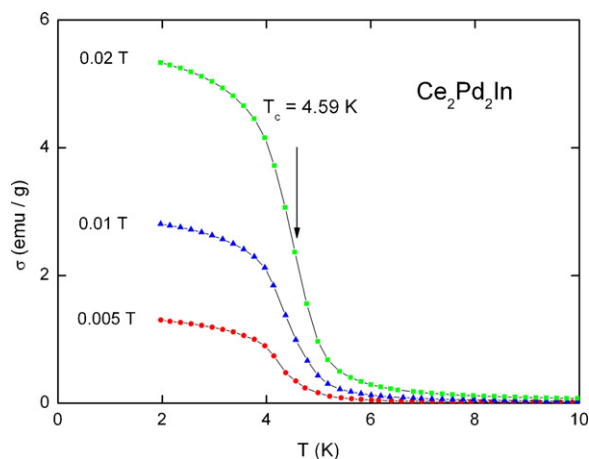


Fig. 4. Low-temperature dependencies of the magnetization in the parent material $\text{Ce}_2\text{Pd}_2\text{In}$, measured in magnetic fields of 0.005, 0.01 and 0.02 T upon cooling the specimen in zero field. The arrow marks the ferromagnetic phase transition.

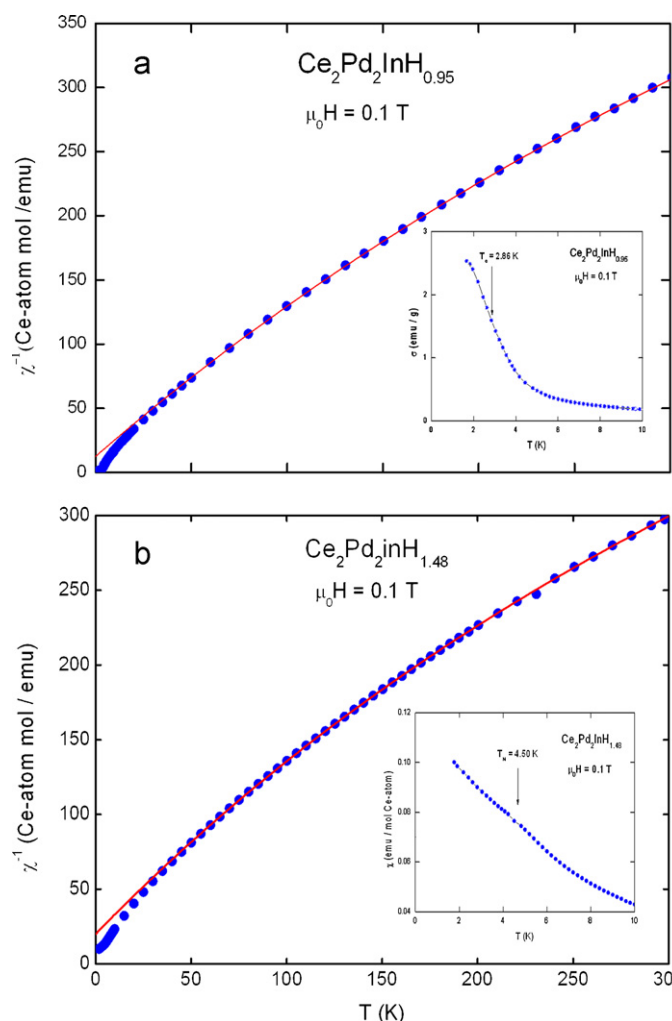


Fig. 5. Temperature variations of the inverse molar magnetic susceptibility of (a) $\text{Ce}_2\text{Pd}_2\text{InH}_{0.95}$ and (b) $\text{Ce}_2\text{Pd}_2\text{InH}_{1.48}$, measured in a magnetic field of 0.1 T. The solid lines represent the MCW fits discussed in the text. The insets display the low-temperature dependencies of the magnetization. The arrows mark the magnetic phase transition.

these samples gradually decreases with raising the hydrogen content. Simultaneously, one observes a systematic decrease in the value of magnetization measured deep in the ordered state. In contrast, hardly any change was observed in the paramagnetic region. Above about 50 K, the inverse magnetic susceptibility of all these alloys can be described by means of the so-called modified Curie–Weiss (MCW) law, $\chi = \chi_0 + C/(T - \theta_p)$, with the effective magnetic moment $\mu_{\text{eff}} = \sqrt{8C}$ of about $2.43\mu_B$, the paramagnetic Curie temperature θ_p close to -13 K , and the Van Vleck contribution χ_0 of the order of $10^{-3}\text{ emu}/(\text{mol Ce-atom})$ (values averaged over the results obtained for the measured hydrides). At lower temperatures some deviations from the MCW formula were found, which presumably arise due to crystalline field (CF) interactions.

As an example, Fig. 5a presents the magnetic behaviour in $\text{Ce}_2\text{Pd}_2\text{InH}_{0.95}$, for which the derived MCW parameters are $\mu_{\text{eff}} = 2.46(3)\mu_B$, $\theta_p = -9(1)\text{ K}$, and $\chi_0 = 8.3(3) \times 10^{-4}\text{ emu}/(\text{mol Ce-atom})$. The Curie temperature for this sample, determined as an inflection point on the $\sigma(T)$ curve, is $T_C = 2.8(5)\text{ K}$, while the magnetization measured at 1.8 K in a field of 0.1 T amounts to 2.8 emu/g, i.e. it is strongly reduced in respect to that in the parent compound. Actually, as shown in Fig. 6a, the magnetization measured in $\mu_0 H = 5\text{ T}$ systematically decreases with increasing the hydrogen

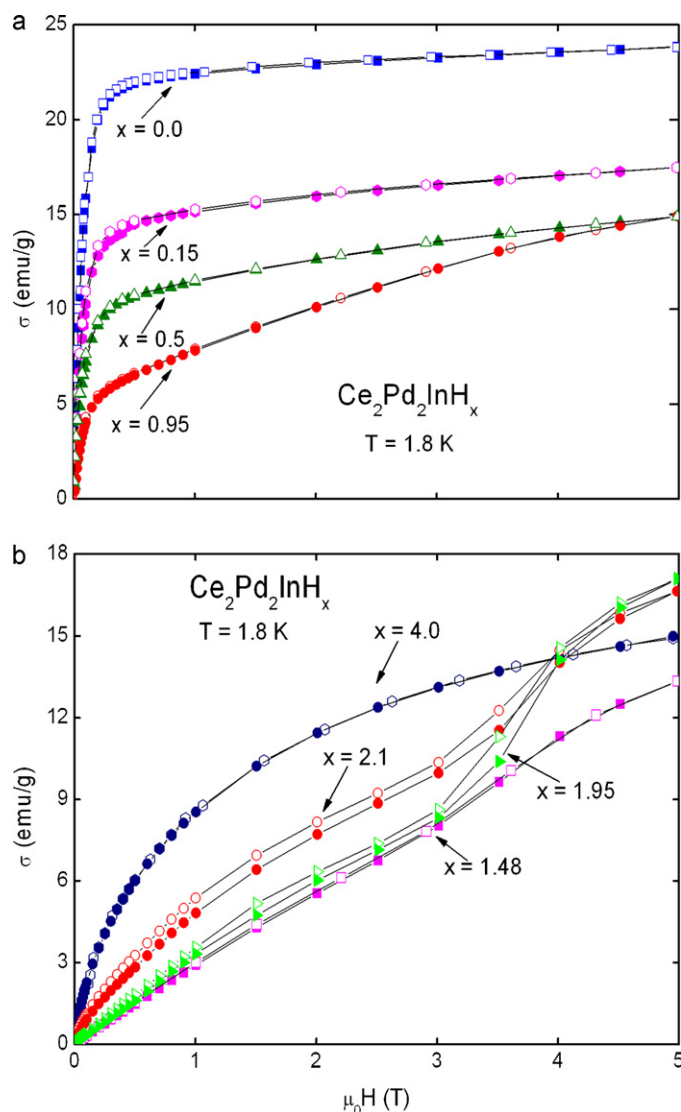


Fig. 6. Field dependencies of the magnetization of $\text{Ce}_2\text{Pd}_2\text{InH}_x$ with the hydrogen content (a) $x < 1.0$ and (b) $1.48 \leq x \leq 4.0$, taken at 1.8 K with increasing (full symbols) and decreasing (open symbols) magnetic field.

content, and the overall shape of $\sigma(H)$ curves also varies towards nonappearance of any tendency for saturation.

Fig. 5b displays the magnetic properties of $\text{Ce}_2\text{Pd}_2\text{InH}_{1.48}$. Spectacularly, in contrast to all the hydrides with smaller x , no ferromagnetic behaviour is observed at low temperatures. Instead, a small feature occurs on the $\chi(T)$ dependence that might hint at the onset of antiferromagnetic state. The scenario of antiferromagnetic ordering in this compound seems supported by the characteristic variation of its magnetization as a function of the magnetic field strength. As can be inferred from Fig. 6b, the $\sigma(H)$ isotherm taken at 1.8 K is nearly linear up to a field of about 3 T, and then exhibits a clear metamagnetic-like anomaly. Similar behaviour of the magnetization was found for a few other $\text{Ce}_2\text{Pd}_2\text{InH}_x$ hydrides with $1.48 < x \leq 2.49$. Sometimes, a narrow hysteresis in $\sigma(H)$ was additionally observed (see Fig. 6b) that might be associated with little contamination of the sample studied by a ferromagnetic hydride with $x < 1.48$.

Another evidence for the antiferromagnetic ground state in the hydrides with $1.48 \leq x \leq 2.49$ comes from the behaviour of the low-temperature magnetic susceptibility measured in various magnetic fields. As exemplified in Fig. 7 for $\text{Ce}_2\text{Pd}_2\text{InH}_{1.95}$, with rising the field

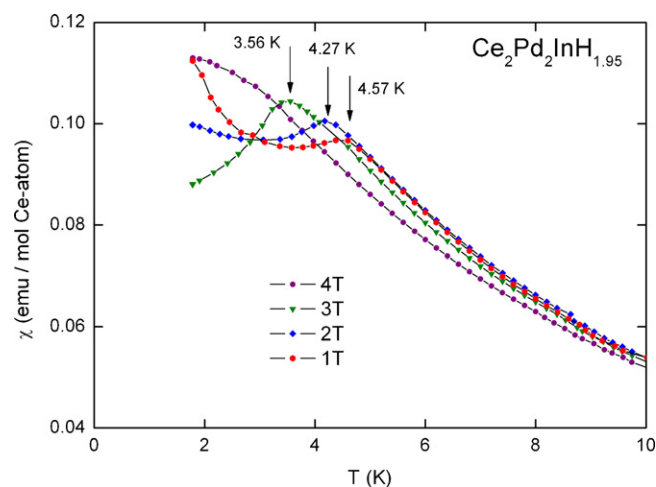


Fig. 7. Low-temperature dependencies of the molar magnetic susceptibility of $\text{Ce}_2\text{Pd}_2\text{InH}_{1.95}$, measured in magnetic fields of 1, 2, 3 and 4 T upon cooling the specimen in zero field. The arrows mark the antiferromagnetic phase transition.

strength the maximum in $\chi(T)$ moves towards lower temperatures, just as expected for antiferromagnets. At $\mu_0 H = 4$ T, i.e. above the metamagnetic critical field, the maximum is completely washed out as the compound is in a field-induced ferromagnetic state.

Contrary to the Curie temperature of the hydrides with $x < 1.48$, the Neel temperature of the materials with $1.48 \leq x \leq 2.49$ seems to be nearly independent of x and amounts to $T_N = 4.6(2)$ K. Moreover, the MCW parameters derived for these alloys hardly change with varying the hydrogen content. For $\text{Ce}_2\text{Pd}_2\text{InH}_{1.48}$ shown in Fig. 5b, the following values were derived by least-square fitting of the MCW formula to the data above 50 K: $\mu_{\text{eff}} = 2.42(2)\mu_B$, $\theta_p = -15(1)$ K, and $\chi_0 = 1.0(2) \times 10^{-3}$ emu/(mol Ce-atom). It is worthwhile noting that these values are nearly same as those found for the hydrides with smaller x .

As the $\text{Ce}_2\text{Pd}_2\text{InH}_x$ hydrides with $x > 2.5$ appeared to be multi-phase materials no attempt was made to measure their magnetic properties. However, such a measurement was performed for the terminal hydride $\text{Ce}_2\text{Pd}_2\text{InH}_{4.0}$, which exhibits amorphous character. As may be inferred from Fig. 8, this compound is paramagnetic down to 1.8 K, and its magnetic susceptibility can be described above 50 K by the MCW law. The so-obtained parameters:

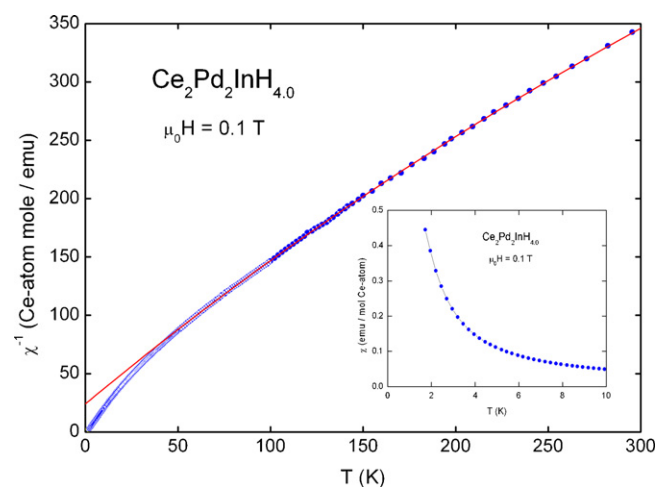


Fig. 8. Temperature variations of the inverse molar magnetic susceptibility of $\text{Ce}_2\text{Pd}_2\text{InH}_{4.0}$, measured in a magnetic field of 0.1 T. The solid line represents the MCW fit discussed in the text. The inset displays the low-temperature dependence of the magnetic susceptibility.

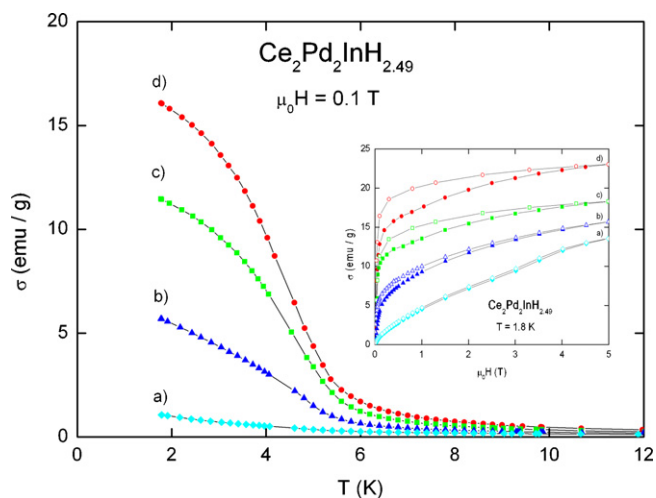


Fig. 9. Low-temperature dependencies of the magnetization of $\text{Ce}_2\text{Pd}_2\text{InH}_{2.49}$ measured in a field of 0.1 T upon cooling the specimen in zero field (a) immediately after synthesis, and after (b) one day, (c) three days, and (d) one week of exposure to air. The inset shows the field variations of the magnetization taken at 1.8 K with increasing (full symbols) and decreasing (open symbols) magnetic field after the time periods as in the main panel.

$\mu_{\text{eff}} = 2.43(3)\mu_B$, $\theta_p = -18(1)\text{ K}$, and $\chi_0 = 1.6(4) \times 10^{-3} \text{ emu}/(\text{mol Ce-atom})$ are very similar to those derived for the other hydrides.

4. Summary

The compound $\text{Ce}_2\text{Pd}_2\text{In}$ was found to easily absorb hydrogen at moderate conditions of pressure and temperature, but its hydrides are very unstable and rapidly decompose in air to a hydride $\text{Ce}_2\text{Pd}_2\text{InH}_x$ with $x \approx 0.07$. For the hydrogen content $x \leq 2.5$, the primitive tetragonal structure of the Mo_2FeB_2 -type, adopted by the parent compound, is retained, while a nearly isotropic expansion of the unit cell occurs. The higher hydrides contain impurity phases, mainly CeH_2 , amount of which increases with rising the hydrogen content. Close to $x = 4$ only amorphous samples are formed.

The $\text{Ce}_2\text{Pd}_2\text{InH}_x$ hydrides exhibit localized magnetism due to fairly stable $4f^1$ electronic configuration of the trivalent Ce ions. All the samples with $x < 1.48$ order ferromagnetically with the Curie temperature and the ordered magnetic moment both gradually decreasing with increasing the hydrogen content. In contrast, for the samples with $1.48 \leq x < 2.5$, antiferromagnetic ordering was found below $T_N = 4.6\text{ K}$ that seems fairly independent of x . The observed change in the character of the magnetic ground state may be rationalized by oscillating nature of the Rudermann–Kittel–Kasuya–Yosida (RKKY) exchange interactions

that presumably govern the magnetic behaviour in these compounds. Hydrogenation affects the RKKY coupling between the magnetic Ce ions by both changing their spacing in the crystal lattice and filling the conduction band with additional electrons.

More detailed characterization of the magnetic properties of the $\text{Ce}_2\text{Pd}_2\text{InH}_x$ system, preferably by means of neutron diffraction studies on the corresponding deuterides, may be hampered by highly unstable nature of the specimens. The rate of spontaneous decomposition of the hydrides appears to be strongly dependent on the initial hydrogen content in a given sample, namely the larger x the faster deterioration takes place. Accordingly, one may observe a change in the magnetic properties as a function of time. As an example, Fig. 9 demonstrates the evolution in the magnetic characteristics of a sample with the initial composition $\text{Ce}_2\text{Pd}_2\text{InH}_{2.49}$. Apparently, both the temperature and field dependencies of the magnetization markedly vary with the time passing from removal of the specimen from the reaction chamber. In particular, the $\sigma(H)$ function measured immediately after synthesis (the curve labelled a) closely resembles those presented in Fig. 6b for the hydrides $\text{Ce}_2\text{Pd}_2\text{InH}_{1.48}$, $\text{Ce}_2\text{Pd}_2\text{InH}_{1.95}$ and $\text{Ce}_2\text{Pd}_2\text{InH}_{2.1}$ with antiferromagnetic ground states, but then it transforms into ferromagnetic-like behaviour (the curve labelled b) already after one day of exposure to air (compare Fig. 6a). In subsequent measurements, made after three and seven days after the synthesis, respectively (the curves labelled c and d), one observes a gradual rise in the magnitude of the magnetization measured at 1.8 K. In parallel, one finds corresponding changes in the $\sigma(T)$ variations, which seemingly transform in their shapes from the antiferromagnetic- to ferromagnetic-like type.¹ In overall, the features presented in Fig. 9, illustrate the modifications in the magnetic nature of the ground state in $\text{Ce}_2\text{Pd}_2\text{InH}_{2.49}$, which accompany the process of gradual hydrogen escape from the studied material.

References

- [1] D. Kaczorowski, P. Rogl, K. Hiebl, *Phys. Rev. B* 54 (1996) 9891.
- [2] R. Hauser, H. Michor, E. Bauer, G. Hilscher, D. Kaczorowski, *Physica B* 230–232 (1997) 211.
- [3] F. Hulliger, B.Z. Xue, *J. Alloys Compd.* 215 (1994) 267.
- [4] R.A. Gordon, Y. Ijiri, C.M. Spencer, F.J. DiSalvo, *J. Alloys Compd.* 224 (1995) 101.
- [5] Y. Ijiri, F.J. DiSalvo, *J. Alloys Compd.* 233 (1996) 69.
- [6] D. Kaczorowski, M. Giovannini, R. Hauser, H. Michor, E. Bauer, G. Hilscher, *Czech. J. Phys.* 46 (1996) 2063.
- [7] F. Furgeot, P. Gravereau, B. Chevalier, L. Fournes, J. Etourneau, *J. Alloys Compd.* 238 (1996) 102.
- [8] R. Mallik, E.V. Sampathkumaran, J. Dumschat, G. Wortmann, *Solid State Commun.* 102 (1997) 59.
- [9] M. Giovannini, H. Michor, E. Bauer, G. Hilscher, P. Rogl, W. Sikora, A. Saccone, R. Ferro, *Phys. Rev. B* 61 (2000) 4044.
- [10] W. Iwasieczko, D. Kaczorowski, *J. Alloys Compd.* 507 (2010) 376.
- [11] A. Boulfif, D. Louer, *J. Appl. Crystallogr.* 37 (2004) 724.
- [12] W. Iwasieczko, D. Kaczorowski, *J. Alloys Compd.*, to be submitted for publication.

¹ Actually, the $\sigma(T)$ curve labelled a in the main panel of Fig. 9 is similar to that presented in Fig. 5b for the antiferromagnetic hydride $\text{Ce}_2\text{Pd}_2\text{InH}_{1.48}$. Rather vague evidence for the antiferromagnetic phase transition in $\text{Ce}_2\text{Pd}_2\text{InH}_{2.49}$ is likely a consequence of partial deterioration of the nominally “fresh” sample.